# Supporting Information
# Degron-based bioPROTACs for controlling signaling in CAR T cells

**Authors**:
Matthew S. Kim[1,2,3], Hersh K. Bhargava[2,3,4], Gavin E. Shavey[2,5], Wendell A. Lim[2,6], Hana El-Samad*[2,3,7,8], Andrew H. Ng[2,6,9]*

**Affiliations:**

1. Tetrad Graduate Program, University of California San Francisco, San Francisco, CA, 94158, USA
2. Cell Design Institute, University of California San Francisco, San Francisco, CA, 94158, USA
3. Department of Biochemistry and Biophysics, University of California San Francisco, San Francisco, CA, 94158, USA
4. Biophysics Graduate Program, University of California San Francisco, San Francisco, CA, 94158, USA
5. Current affiliation: Arsenal Biosciences Inc., South San Francisco, CA, 94080, USA
6. Department of Cellular and Molecular Pharmacology, University of California San Francisco, San Francisco, CA, 94158, USA
7. Chan-Zuckerberg Biohub, San Francisco, CA, 94158, USA
8. Current affiliation: Altos Labs Inc., Redwood City, CA, 94065, USA
9. Current affiliation: Department of Molecular Biology, Genentech Inc., South San Francisco, CA, 94080, USA

* co-corresponding authors

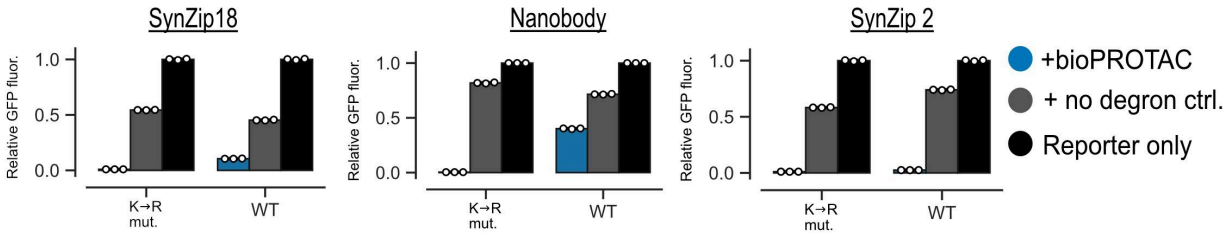


Figure S1. **Mutation of lysine residues to arginine of bioPROTAC binding domains improves degradation activity** GFP fluorescence was measured by flow cytometry. Relative GFP fluorescence is calculated as described in Fig 1. Labels above plots describe the binding domain used by each bioPROTAC. Dots represent technical replicates and error bars show SEM. Data is representative of three independent experiments.

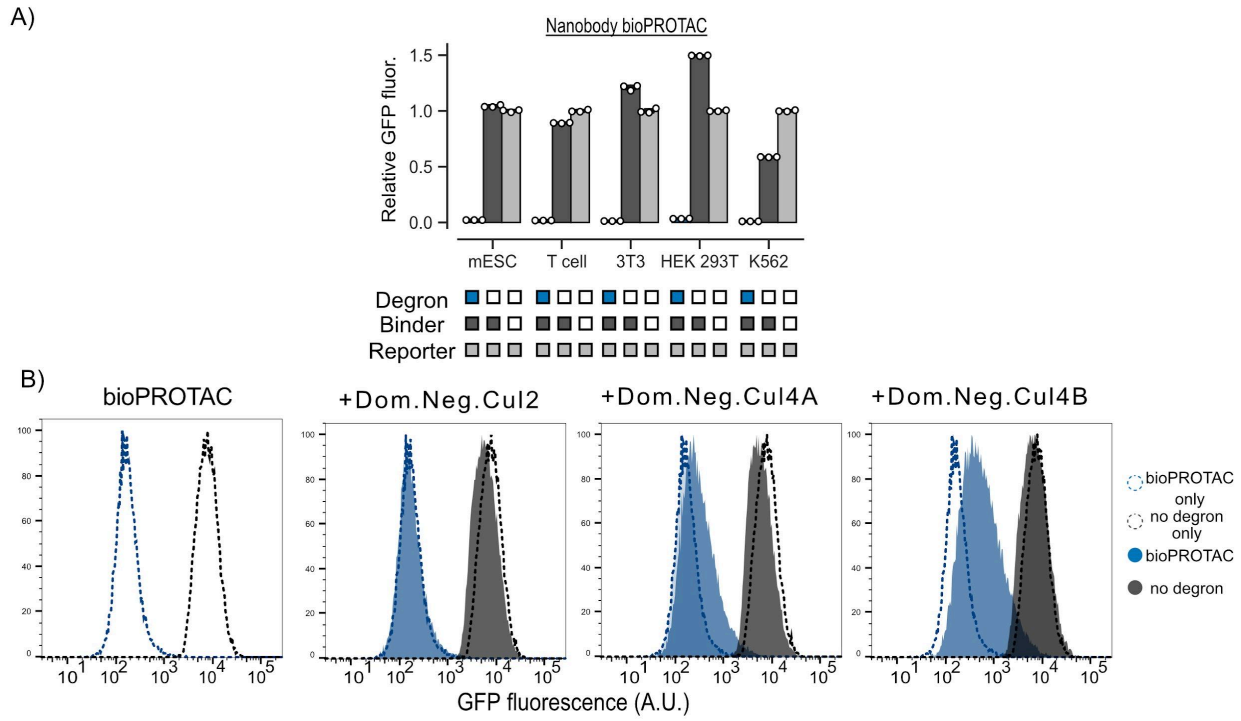


Figure S2. **Characterization of bioPROTAC mechanism and function** (A) The vhhGFP4 nanobody bioPROTAC showed potent degradation across all tested mammalian cell lines. GFP fluorescence was measured by flow cytometry. Relative GFP fluorescence is calculated as described in Fig 1. Dots represent technical replicates and error bars show SEM.
(B) Dominant negative cullin ring ligases from the Cul4 family rescued SynZip18 bioPROTAC degradation. GFP fluorescence was measured by flow cytometry. Plots are representative of three biological replicates.

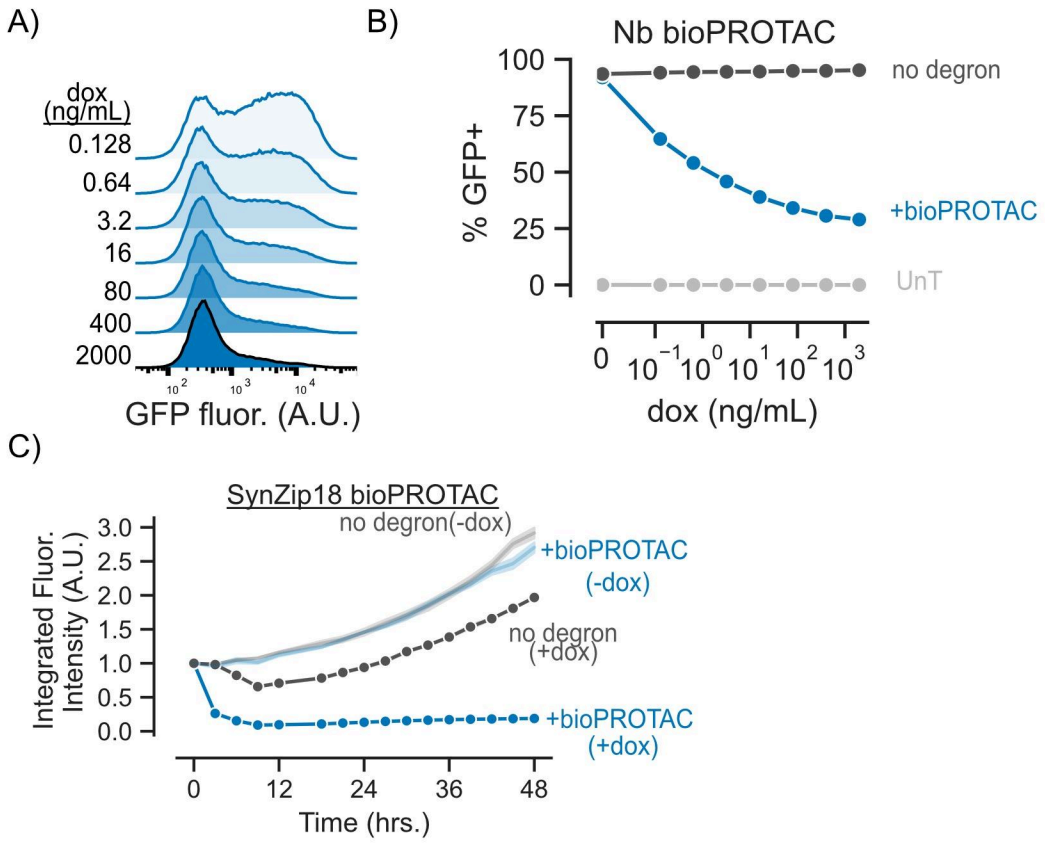


Figure S3. **Further characterization of bioPROTAC degradation kinetics** (A) Flow cytometry histograms of doxycycline inducible bioPROTAC against GFP target following 48 hours of treatment with doxycycline. The data shown here are selected from cells that are positive for BFP, a marker for transcriptional activation by doxycycline. These data are representative of three biological replicates. (B) The vhhGFP4 nanobody bioPROTAC showed dose-dependent degradation. bioPROTACs titration results in dose-dependent degradation of cytosolic proteins. Jurkat T cells were lentivirally transduced with a GFP reporter protein and a plasmid encoding a doxycycline inducible nanobody bioPROTAC and the Tet3G protein. After isolation by FACS, cells were treated with a 5-fold titration series of dox starting at 2000 ng/mL or a media only control for 48 hours. bioPROTAC efficacy was assessed by flow cytometry. Each dot is the mean of three biological replicates. Error show SEM. (C) Time traces of doxycycline-inducible SynZip bioPROTAC degradation with additional controls. Jurkat cells expressing doxycycline-inducible SynZip bioPROTAC and a GFP reporter were treated with 2000 ng/mL doxycycline and GFP fluorescence was measured over time for 48 hours. GFP fluorescence measurements were captured by fluorescence microscopy and live cell imaging on

an Incucyte machine. Data was analyzed in the Incucyte software. Data is normalized to the values at the initial time point for each condition.

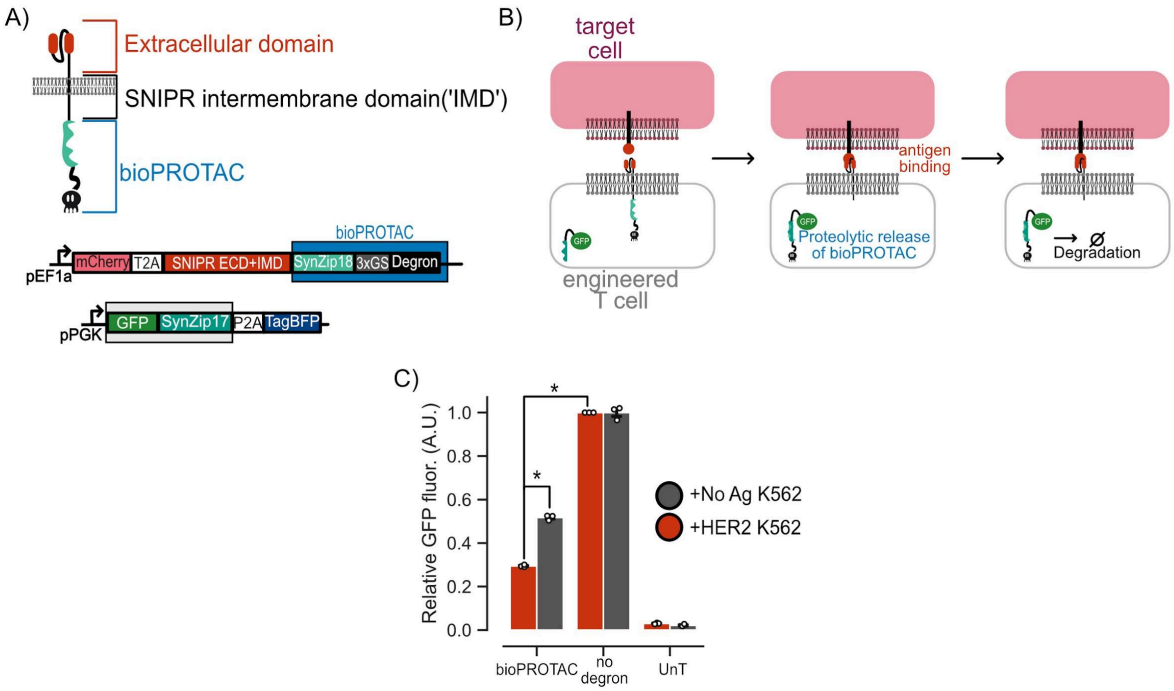


Figure S4. **Combining bioPROTACs with the extracellular and intermembrane domains of SNIPR creates an antigen inducible targeted protein degradation tool** (A) Cartoon schematic of domain swap of transcription factor domain of SNIPR to SynZip18 bioPROTAC to create antigen inducible degradation tool. CD4+ primary human T cells were transduced with the diagrammed lentiviral payloads. Engineered T cells were then co-cultured with HER2 expressing K562s or no antigen K562s for 72 hours at 1:1 E:T ratio. SNIPR-bioPROTAC fusion protein activity was measured by changes in GFP fluorescence by flow cytometry. (B) Cartoon depicting proposed mechanism of SNIPR-bioPROTAC fusion protein. (C) . SNIPR-bioPROTAC fusion is capable of antigen induced GFP degradation despite moderate levels of antigen independent degradation. GFP fluorescence was measured by flow cytometry. Relative GFP fluorescence was calculated by normalizing each test condition to a reporter only control. Each dot represents a technical replicate and error bars show SEM. Significance determined by unpaired t-test, * = P < .01

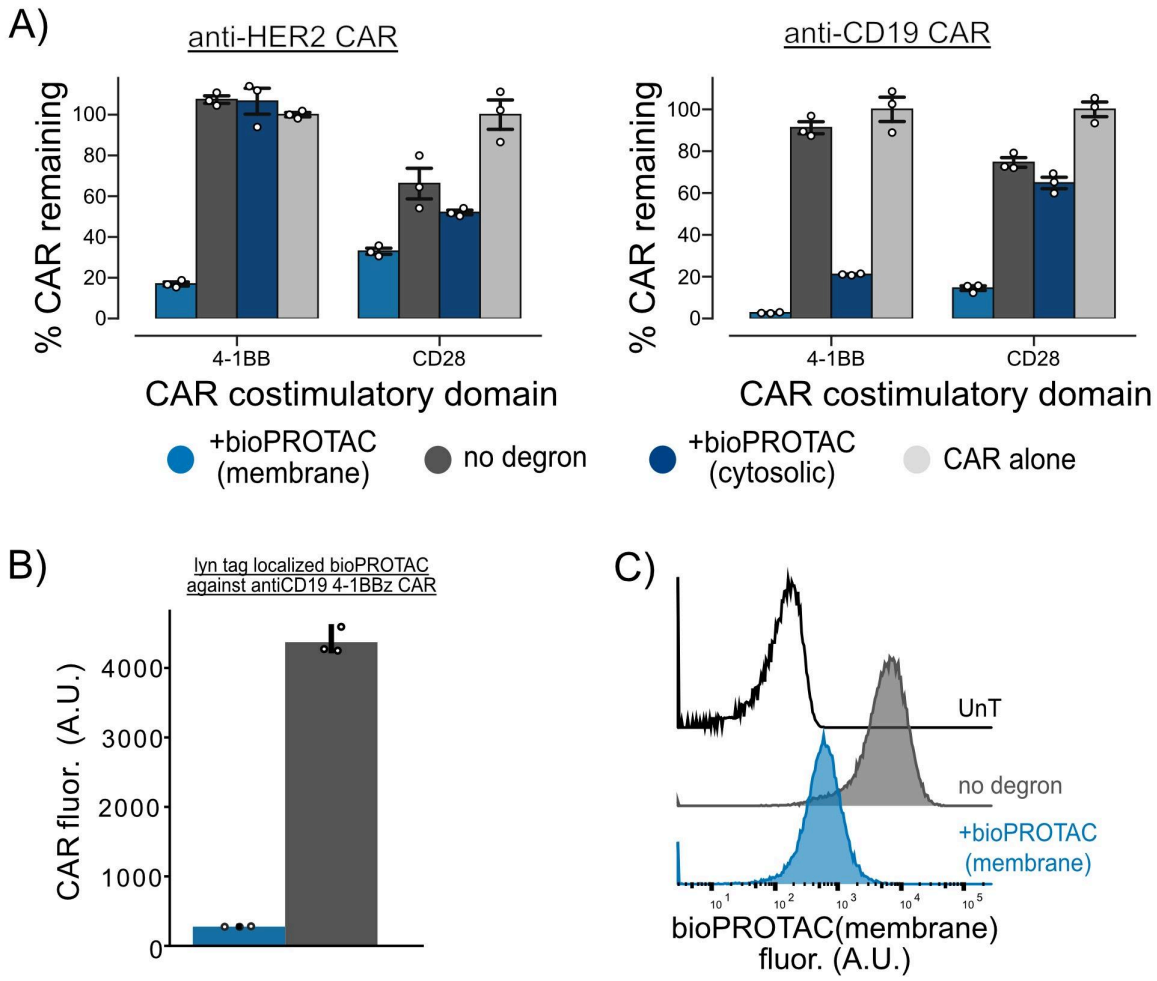


Figure S5. **bioPROTAC(membrane) characterization.** (A) bioPROTAC(membrane) degradation performs better against second-generation CARs with 4-1BB than those with CD28 costimulatory domains. Jurkat T cells were transduced via lentivirus with plasmids encoding a second-generation CAR and a bioPROTAC(membrane) as described in Figure 3A. CAR expression was measured by staining for an extracellular tag fused to the CAR and measured by flow cytometry. % CAR remaining was calculated as described in Fig 3. Each dot represents technical replicates and error shows SEM. (B) bioPROTAC(membrane) can be recruited to the membrane with different domains without loss of function. Jurkat T cells were engineered to express an antiCD19 4-1BBz CAR. Then, either a lyn tagged bioPROTAC(membrane) or a lyn tagged no degron control was introduced by lentivirus. CAR expression levels were assessed by antibody stain for an extracellular tag. Each dot represents technical replicates and error shows SEM. (C) Flow cytometry histograms representing DAP10 bioPROTAC(membrane) expression in Jurkat T cells. bioPROTAC(membrane) fluorescence values were measured by immunofluorescence staining for a V5 tag fused to the extracellular domain of the protein followed by flow cytometry. Plots are representative of three technical replicates.

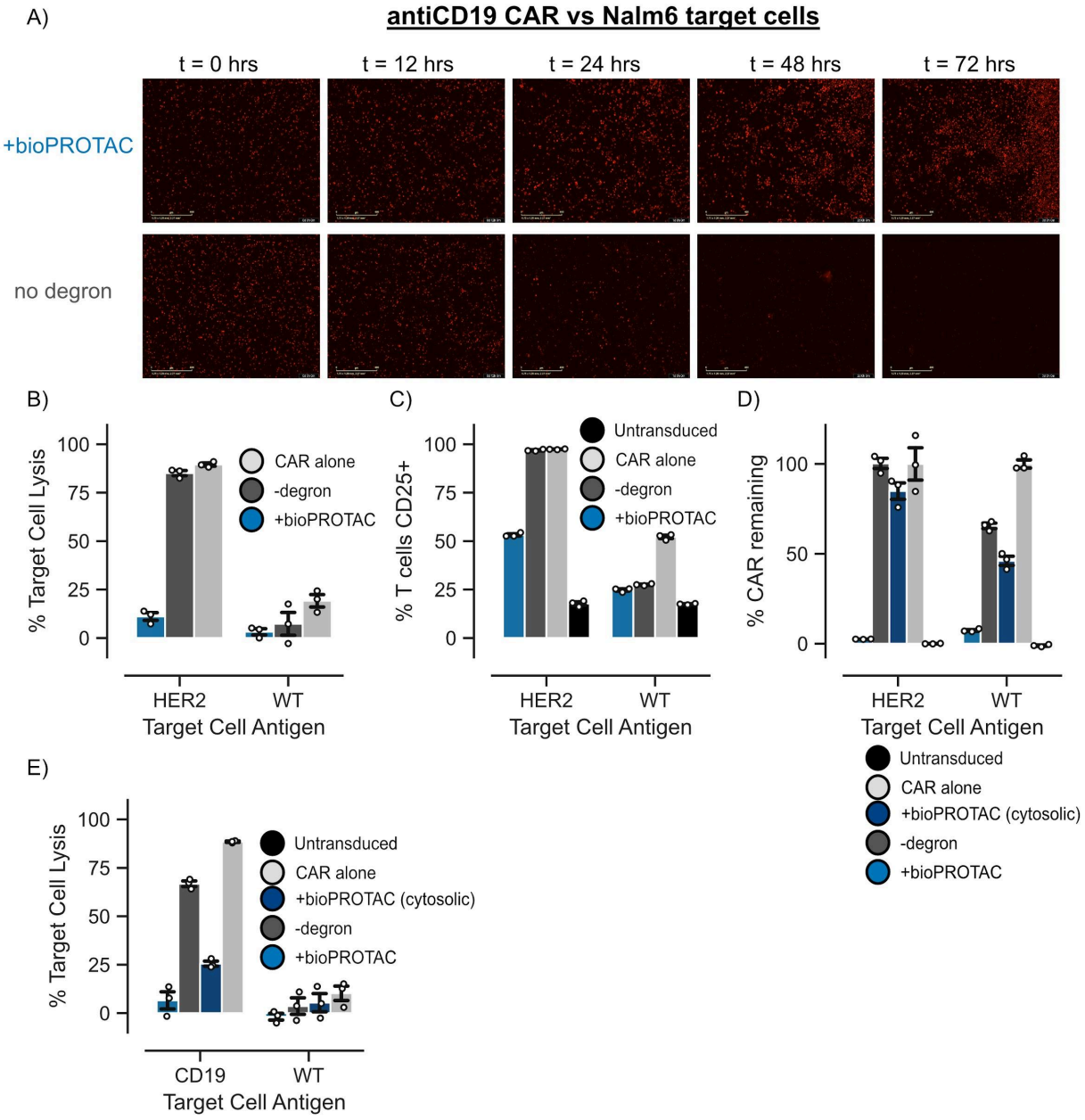


Figure S6. **Further characterization of bioPROTAC(membrane) control of CARs.** (A) Representative images of live cell imaging of target cell lysis by CAR T cells co-cultured with mCherry+ Nalm6 cells. Images were taken on an Incucyte machine. (B) bioPROTAC(membrane) impaired anti-HER2 4-1BBz CAR cytotoxicity. Cell lysis was calculated using cell counts measured by flow cytometry and normalized to cell counts of UnT cells against each target cell type. Dots represent technical replicates and error bars show SEM. (C) Coexpression of bioPROTAC(membrane) prevented anti-HER2 4-1BBz CAR associated activation of CD25. CD25 levels were measured by immunostaining followed by flow cytometry. Dots represent technical replicates and error bars show SEM. (D)

bioPROTAC(membrane) induced internalization of anti-HER2 4-1BBz CAR. CAR fluorescence was measured by immunostaining followed by flow cytometry. Dots represent technical replicates and error bars show SEM. (E) Membrane localization is required for strong ablation of anti-CD19 4-1BBz CAR induced cytotoxicity in primary T cells. Same data as Figure 4B including a control with a cytosolic bioPROTAC. Each dot represents technical replicates and error shows SEM.

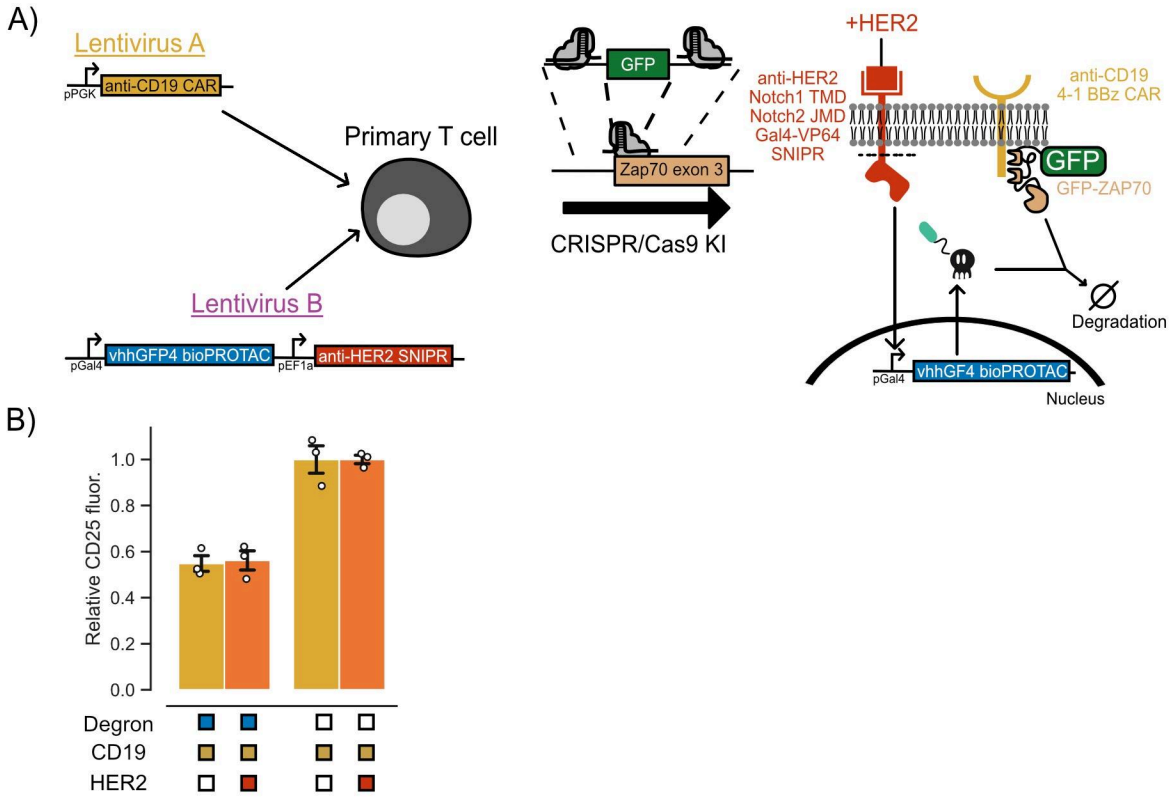


Figure S7. **bioPROTAC circuit characterization** (A) Cartoon depiction of bioPROTAC circuit engineering strategy and circuit function. (B) CD25 levels of bioPROTAC expressing engineered T cells were assessed by antibody stain after 48 hours of co-culture with CD19 or CD19 and HER2 expressing K562 cells. CD25 fluorescence levels were measured by flow cytometry. Relative CD25 levels were calculated by normalizing each test condition to a no degron control. Each dot represents a technical replicate. Error bars show SEM.